

Confined LO phonons in superlattices with interfacial broadening

This article has been downloaded from IOPscience. Please scroll down to see the full text article.

1992 J. Phys.: Condens. Matter 4 4509

(<http://iopscience.iop.org/0953-8984/4/18/017>)

View [the table of contents for this issue](#), or go to the [journal homepage](#) for more

Download details:

IP Address: 171.66.16.159

The article was downloaded on 12/05/2010 at 11:54

Please note that [terms and conditions apply](#).

Confined LO phonons in superlattices with interfacial broadening

M I Vasilevskiy

Department of Physics, University of Essex, Wivenhoe Park, Colchester, CO4 3SQ, UK

Received 27 August 1991

Abstract. A 1D lattice dynamics model for superlattices (SL) is developed to investigate the consequences of interfacial broadening on the confined optical phonons. It is shown that simple results can be obtained for two cases when the alloy of the substances that construct the SL displays either explicit two-mode behaviour (for instance, AlGaAs) or an intermediate type of optical behaviour. In the latter case, the modes of two optical subbands move towards each other, and δ -like peaks of the phonon density of states broaden into the Gaussian-like curves. In contrast, for AlAs/GaAs SL, the modes of both the AlAs-like and GaAs-like subbands move downwards and broaden asymmetrically. The shape of the lines is sensitive to the composition profile.

1. Introduction

The lattice dynamics of semiconductor superlattices (SL) with application to those with non-abrupt interfaces has recently attracted much attention [1–8]. The need for a good understanding of this imperfect influence on the SL vibrations arises partly because phonons are known to influence a number of electronic properties. In addition, detection of the phonons through Raman spectroscopy should be a good probe for alloy disorder [5, 6].

The problem of calculating the effects of interface broadening has been considered either using a 1D model [5, 8] or one involving full 3D lattice dynamics [3, 4, 6, 7]. The latter must be used for ultrathin SL (see [7]), but the 1D lattice dynamics model gives a good quantitative description of the effect for phonons propagating along the (100) axis of $(\text{GaAs})_{n_1}(\text{AlAs})_{n_2}$ SL with moderately small n_1 and n_2 [4, 8]. Since a 1D model is obviously easier from the computational point of view, its advantages are clear. Unfortunately, the successful model [8] is based on the intuitive state of susceptibility average for disordered atomic planes, and the degree of generality of this approach is unclear so far. On the other hand, the 1D model of [5], which starts 'from first principles', leads to results inconsistent with experimental data.

In the present paper, we are trying to shed further light on the application of the linear chain model to the problem of the confined LO mode shift due to the interface non-abruptness. We will be able to link the controversial results [5, 8], and to give simple formulae for the shift and for the line broadening of these modes.

2. 1D lattice dynamics for SL

We start by writing down the Hamiltonian of the chain modelling the SL:

$$H = \frac{1}{2} \sum_{\substack{l,j \\ l',j'}} V_l^{(j)} V_{l'}^{(j')} F \begin{pmatrix} l, l' \\ j, j' \end{pmatrix} + \frac{1}{2} \sum_{l,j} \dot{V}_l^{(j)} \dot{V}_l^{(j)} M_l^{(j)} \quad (1)$$

where $l = 1, 2, \dots, nN$ is a number of a unit cell, $j = 0, 1$ labels atom types (anion or cation) in the unit cell, $n = n_1 + n_2$, N is the number of SL periods, $M_l^{(j)}$ and $V_l^{(j)}$ are atomic masses and longitudinal displacements respectively, and F is a strength matrix. Let us confine ourselves by considering fluctuations that are coherent in the different periods of the SL. It is reasonable to introduce variables $\xi = 1, \dots, n$ and $m = 1, \dots, N$ so that $l = \xi + mn$. Representing $V_l^{(j)}$ in the form

$$V_l^{(j)} = \frac{1}{\sqrt{M_\xi^{(j)} N}} \sum_Q \left\{ U_\xi^{(j)}(Q) e^{iQmn} + U_\xi^{(j)}(-Q) e^{-iQmn} \right\} \quad (2)$$

and substituting (2) into (1) we obtain

$$H = \frac{1}{2} \sum_{\substack{\xi, \xi' \\ j, j'}} \sum_Q \left\{ U_\xi^{(j)}(Q) U_{\xi'}^{(j')}(-Q) \frac{F_{\xi\xi'}^{jj'}(Q)}{\sqrt{M_\xi^{(j)} M_{\xi'}^{(j')}}} + \dot{U}_\xi^{(j)}(Q) \dot{U}_{\xi'}^{(j')}(-Q) \right\} \quad (3)$$

where

$$F_{\xi\xi'}^{jj'}(Q) = \frac{1}{N} \sum_{\substack{m=1 \\ m'=1}}^N F \begin{pmatrix} \xi + mn, & \xi' + m'n \\ j, & j' \end{pmatrix} e^{-iQn(m-m')}.$$

The equation of motion for the Green function $G_{\xi\xi'}^{jj'}(Q)$ which follows from (3) is

$$(w_\xi^{(j)} - \omega^2) G_{\xi\xi''}^{jj''}(Q) = \delta_{jj''} \delta_{\xi\xi''} - \sum_{j', \xi'} W_{\xi\xi'}^{jj''}(Q) G_{\xi'\xi''}^{j'j''}(Q) \quad (4)$$

where

$$w_\xi^{(j)} = F_0 / M_\xi^{(j)} \quad (5)$$

$$W_{\xi\xi'}^{jj'} = F_{1\xi\xi'}^{jj'} / \sqrt{M_\xi^{(j)} M_{\xi'}^{(j')}} \quad (6)$$

$$F_0 \delta_{\xi\xi'} \delta_{jj'} + F_{1\xi\xi'}^{jj'} = F_{\xi\xi'}^{jj'}. \quad (6)$$

Introducing a locator [9]

$$g_{\xi\xi'}^{jj'} = g_\xi^{(j)} \delta_{\xi\xi'} \delta_{jj'}, \quad g_\xi^{(j)} = 1 / (w_\xi^{(j)} - \omega^2) \quad (7)$$

we can write down the Dyson equation [9]:

$$G_{\xi\xi'}^{jj'} = g_{\xi\xi'}^{jj'} - g_{\xi\xi''}^{jj''} W_{\xi''\xi'''}^{j''j'''} G_{\xi'''\xi'}^{j'''j'}. \tag{8}$$

Of course, (8) can be rewritten in any representation. In the ideal SL the eigenfunction corresponding to a confined optical phonon of wavenumber k is (see, for example, [10]):

$$U_{\xi}^{(j)} = \begin{cases} \begin{pmatrix} 1 \\ \alpha_1 \end{pmatrix} A_1 \sin(\tilde{k}_1 \xi) & \xi \leq n_1 \\ 0 & \xi > n_1 \end{cases} \tag{9}$$

for the lower optical subband (for instance, GaAs-like) and

$$U_{\xi}^{(j)} = \begin{cases} 0 & \xi \leq n_1 \\ \begin{pmatrix} 1 \\ \alpha_2 \end{pmatrix} A_2 \sin(\tilde{k}_2 \xi) & \xi > n_1 \end{cases} \tag{9'}$$

for the upper one (Al-As-like), where

$$\begin{aligned} \alpha_s &= (F_0 - M_0 \omega^2) / F_0 \cos \tilde{k}_s \\ A_s &= \sqrt{2 / (1 + \alpha_s^2)} \\ \tilde{k}_s &= \pi r / n_s \quad r = 1, \dots, n_s \quad s = 1, 2 \end{aligned} \tag{10}$$

and M_0 is the atomic mass of the anions. The column vector $\begin{pmatrix} 1 \\ \alpha \end{pmatrix}$ represents relative amplitudes of vibrations of two atoms in the unit cell. Since both matrices \hat{g} and \hat{W} are diagonal in this basis, (8) leads to an obvious expression for Green's function:

$$\tilde{G}_{kk} = 1 / (\tilde{g}_{kk}^{-1} + W(k)) \tag{11}$$

for confined phonon states.

In the SL with imperfect interfaces an expression for g_{ξ} (hereafter we omit the superscript $j = 1$ for clarity) can be written as

$$g_{\xi} = \tilde{g}_{\xi} (1 + \beta_{\xi}) \tag{12}$$

where \tilde{g}_{ξ} relates to the ideal SL and the random variable β_{ξ} is

$$\beta_{\xi} = (\omega_1^2 - \omega_2^2)(1 - C_{\xi}) / [\tilde{g}_{\xi}^{-1} - (\omega_1^2 - \omega_2^2)(1 - C_{\xi})] \tag{13}$$

for $\xi \leq n_1$ and

$$\beta_{\xi} = (\omega_2^2 - \omega_1^2) C_{\xi} / [\tilde{g}_{\xi}^{-1} - (\omega_2^2 - \omega_1^2) C_{\xi}] \tag{13'}$$

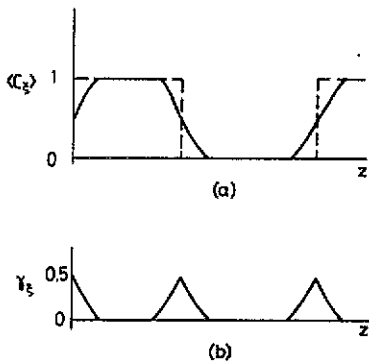


Figure 1. The composition distribution (a) for an ideal SL (broken curve) and for an SL with imperfect interfaces (full curve). (b) A non-ideality parameter.

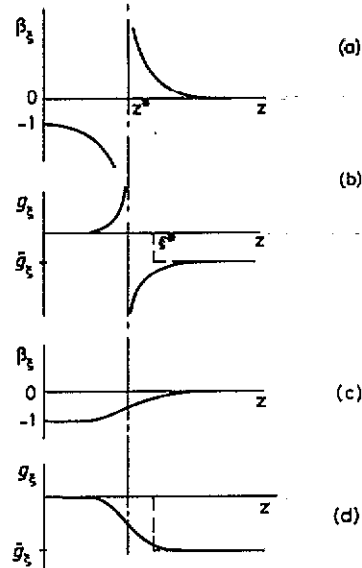


Figure 2. A qualitative picture of the behaviour of β_ξ and g_ξ defined by (13) and (12) respectively for GaAs (a), (b) and AlAs (c), (d) layers. z^* is the solution of (15) taken to be the same for both layers for simplicity, and $\xi^* = [z^*] + 1$. Broken curves show the approximation (14).

for $\xi > n_1$. In (13) we have introduced

$$\omega_s^2 = F_0/M_s \quad s = 1, 2.$$

If $M_0 > M_1$ and M_2 , then ω_s^2 are the squared X-point frequencies of the subbands. The random variable C_ξ appearing in (13) is the concentration of atoms 1 which varies in the range $0 \leq C_\xi \leq 1$ (see figure 1).

As is known, properties of a disordered medium are determined by the averaged Green function [9, 11], so we have to average (8) with g_ξ given by (12) and (13) over all realizations. In principle, each atom of our chain represents the whole (100) plane of the real SL. However, a lateral scale of the averaging should include only atoms within the in-plane localization area of the phonon mode. This scale depends on the average thickness of the layers and on the considered vibration, but in general it is of order 10 Å (this is an experimental estimate) [4]. The exception is the fundamental vibration mode which remains extended up to 100 Å [4].

3. Confined mode shift and broadening

Let us consider two cases:

(i) $|(\omega_2^2 - \omega_1^2) \tilde{g}_\xi| \gg 1$. In this case the alloy of the materials which compose the SL shows an explicit two-mode behaviour, i.e. LO-phonon subbands are strongly

separated compared with the width of each of them [12]. As $\langle C_\xi \rangle$ drops sharply with distance from the interface, we can use the approximation shown in figure 2, that is

$$\beta_\xi = \begin{cases} -1 & \xi < \xi_1 & \xi > n_1 - \xi_1 \\ 0 & \xi_1 < \xi < n_1 - \xi_1 \end{cases} \quad (14)$$

where we have introduced a 'push-out' length $\xi_1 = [z^*] + 1$, and z^* is a solution of the equation

$$|(\omega_1^2 - \omega_2^2) \tilde{g}_\xi (1 - C(z))| = 1 \quad (15)$$

where z is measured in the units of the interplane distance and varies continuously, and $\xi \leq n_1$. Due to approximation (14) $(\langle \beta_\xi \rangle)^p = \langle \beta_\xi^p \rangle$ for any integer p , and (8) for the average Green function leads to the same result (11), since all matrices are of semi-diagonal structure

$$\tilde{g}_{kk'} = \begin{pmatrix} g_{11} & 0 & 0 & 0 & 0 \\ 0 & \ddots & 0 & 0 & 0 \\ 0 & 0 & g_{nn} & 0 & 0 \\ 0 & 0 & 0 & & \\ 0 & 0 & 0 & & g_{kk'}^{(ac)} \end{pmatrix} \quad (16)$$

in the representation (9) with the only change $n_s \rightarrow (n_s - 2\xi_s)$, $s = 1, 2$ (ξ_s is given by the same equation (15) but solved for $\xi > n_1$ with substitute $C(z) \rightarrow 1 - C(z)$). Thus, we have

$$\langle G_{kk} \rangle = \sum_{\xi_s} f(\xi_s) \tilde{G}_{kk}(n_s - 2\xi_s) \quad (17)$$

where $f(\xi_s)$ is a distribution function of ξ_s . The main term in (17) corresponds to $\bar{\xi}_s$ which is given by (15) using an average $C(z)$.

This approximation should be good enough for GaAs/AlAs SL because only 10% of Al in the barrier is sufficient to induce a confinement of the GaAs-like vibration [6]. Thus, the GaAs-like phonons are mostly confined in a region of $(n_1 - 2\bar{\xi}_1)$ monolayers. The frequency shift is given by

$$\overline{\Delta\omega_k^2} = ((d\omega^2/dk)k)_{k=\bar{k}_s} 2\bar{\xi}_s/n_s. \quad (18)$$

Of course, the shift can also be found directly from the dispersion curve. Note that $\Delta\omega^2 < 0$ for both subbands.

Results of the calculations for GaAs-like modes in the SL with $n_1 = 20$, $n_2 = 6$ (investigated experimentally in [1]) are shown in figure 3. We used the bulk GaAs dispersion curves of [13], and the composition profile was taken as

$$\langle C(z) \rangle = \frac{1}{2} \operatorname{erfc}(z/L)$$

with the same L for both kinds of interface. The frequency shift $\Delta\omega = \Delta\omega^2/2\omega$ increases approximately parabolically with increasing wavenumber, and is in good agreement with experimental data of [1] for $L = 1.5$. The agreement becomes worse

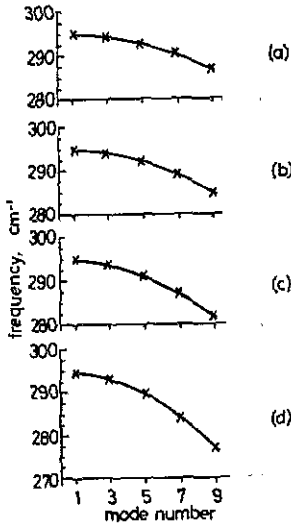


Figure 3. Phonon frequency versus mode number for the GaAs-like subband. The broadening parameter is equal to (a) $L = 0$, (b) $L = 1.5$, (c) $L = 3.5$ and (d) $L = 5.0$. The curves are guides to the eye.

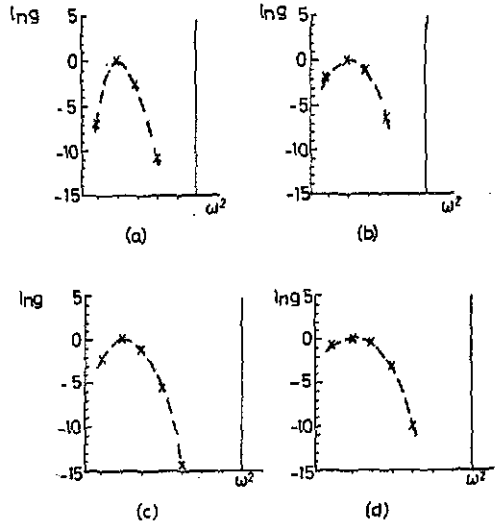


Figure 4. The phonon density of states for the LO_3 GaAs mode for *erfc* ((a), (c)) and *linear* ((b), (d)) composition distribution: (a), (b) $L = 3.5$ and (c), (d) $L = 5.0$. δ -like peaks correspond to the ideal SL. The broken curves are guides to the eye.

as the scale of the broadening increases. For $L = 5$ the shift of the modes 7 and 9 is considerably larger than that observed experimentally [1] after three-hour annealing. There are two reasons for this. First, the 'push-out length' defined as before changes, while the frequency varies over the subband, but it must be taken as the same for all modes of the same subband, otherwise the averaging procedure used above becomes incorrect. This means that the approximation (14) is too crude for larger L . Secondly, a concentration tail of the light impurity in the region of propagation of GaAs-like phonons becomes significant as L increases (see figure 2). Staying strictly within the framework of our model which implies a virtual crystal approximation (VCA) *in plane*, this impurity tail must produce some shift upwards for GaAs-like modes (and vice versa for AlAs-like modes) which also increases with mode number. Unfortunately, the concentration in the tail region is still too high to be treated as a perturbation.

On the other hand, a numerical solution of the equations of motion for the Hamiltonian (3) with $C(z)$ replaced by $\langle C(z) \rangle$ means an averaging of the atomic displacements (random-element isodisplacement approach, see [12] for example), which are not self-averaging values [11].

In general (for a real 3D-lattice) each site is occupied, of course, either by the Ga or by the Al atom, and GaAs-like excitations cannot propagate through the Al occupied sites due to large differences in mass. However, if Ga concentration is higher than the site problem percolation threshold (0.2 for FCC), there should be some propagating states (see [9], for example). For these states, the interfacial broadening might even lead to the increase of the confinement length. A numerical calculation using the supercell Green function approach [14] showed that the propagating states exist in the $Ga_{0.5}Al_{0.5}As$ alloy near the middle of the GaAs-like subband. This fact could be an explanation of a relatively small shift of higher number modes as the broadening increases. However, it is still unclear why the shift dependence on L is

not monotonous for these modes [1].

It is also relevant to note here that the deviation from parabolic dependence of the frequency on the mode number is considered as a variation of the 'effective well' shape from square to parabolic with increasing L [1]. In fact, this is not so since the parabolic well should produce a shift larger than the square shift for both subbands, in contradiction with experiment.

Nevertheless, the simple formula (18) gives correct values of the shift for the first few confined modes unless the interfacial broadening is too large. Now we consider the influence of composition fluctuations on the phonon density of states, which is a number of δ -like peaks in the ideal SL. We use the term 'shape of the line' bearing in mind, for example, non-resonant Raman scattering. Experimental linewidths have been explained as being due to monolayer fluctuations in the layer thickness [2].

The 'shape of the line' is formed by terms in (17) close to $\bar{\xi}_s$. A probability of smaller shift, for example,

$$\Delta\omega_k^2 = \overline{\Delta\omega_k^2} - \epsilon_k$$

where

$$\epsilon_k = (1/n_s)(d\omega^2/dk)k_{k=\bar{k}_s} \tag{19}$$

is the probability of the composition fluctuation when

$$\gamma(z^*) - \delta C(z^*) \simeq \gamma(z^* + 1)$$

where

$$\gamma(z) = \begin{cases} 1 - \langle C(z) \rangle & z \leq n_1 \\ \langle C(z) \rangle & z > n_1 \end{cases}$$

(see figure 1) and

$$\delta C(z) = C(z) - \langle C(z) \rangle.$$

That is,

$$f_{-1} \sim 2 \exp \left\{ - \left[N_p (\gamma(z^*) - \gamma(z^* + 1))^2 \right] / 2\gamma(z^*) (1 - \gamma(z^*)) \right\} \tag{20}$$

and similarly for f_{-2} , etc. N_p in (20) is the number of atoms in a plane within the localization area of the phonon mode, as discussed at the end of the previous section. If the in-plane atomic distribution is not correlated on that scale, we have for the composition fluctuations:

$$\langle \delta C_\xi^2 \rangle = \langle C_\xi \rangle (1 - \langle C_\xi \rangle) / N_p.$$

Considering both the interfaces to be equivalent we obtain (20).

The shift larger than (18) is determined by the fluctuation when

$$\gamma(z^* + 1) + \delta c(z^* + 1) \simeq \gamma(z^*).$$

It is clear that $(f_{+1}/f_{-1}) \ll 1$ because of fast decrease of $\gamma(z)$ with increasing z . In fact, such a fluctuation should be Poissonian:

$$f_{+1} \sim 2 \exp [-\gamma(z^* + 1)N_p \ln \gamma(z^*)/\gamma(z^* + 1)].$$

Thus, we can conclude that in the case (i) of 'two-mode SL' the phonon density of states broadens asymmetrically near the average shift downwards due to the interfacial non-abruptness. Results of the calculations of the 'shape of the line' for the LO_3 GaAs mode using $N_p = 100$ are shown in figure 4 for the erfc-profile (a), (c), and for

$$\langle C(z) \rangle = \frac{1}{2}(1 - z/L)$$

the concentration profile, (b), (d).

The frequency shift between two neighbouring points is 0.52 cm^{-1} for $n_1 = 20$ SL. Thus, we can conclude that the 'shape of the line' is sensitive to the exact impurity distribution along z .

$$(ii) |(\omega_2^2 - \omega_1^2) \tilde{g}_\xi| \lesssim 1.$$

The case (ii) can be regarded as that when the alloy shows an intermediate (between I and II-mode) type of behaviour, GaInAs should be an example [12]. In this case phonons of each of the pure substances can propagate in the alloy of composition x up to some value $1 > x > \frac{1}{2}$, but they are confined in the ideal SL.

Of course, inequality (ii) can hardly be satisfied for the phonon modes near the bottom of each subband. That means that the above consideration can be applied to these modes. On the contrary, for a few first-confined modes, the interfacial broadening can be treated as a perturbation. In terms of figure 2 the situation can be regarded as that when $z^* < 0$.

It is more convenient now to use transformation (2) with

$$\tilde{M}_\xi = \begin{cases} M_1 & \xi \leq n_1 \\ M_2 & \xi > n_1 \end{cases}$$

instead of random M_ξ . This leads to the following expression for the Hamiltonian:

$$H = \tilde{H} - \omega^2 \epsilon_\xi (\gamma_\xi + \delta C_\xi)$$

where

$$\epsilon_\xi = \begin{cases} \epsilon_1 = (M_2 - M_1)/M_1 & \xi \leq n_1 \\ \epsilon_2 = (M_1 - M_2)/M_2 & \xi > n_1. \end{cases}$$

In the VCA corrections to the squared mode frequencies are given by

$$\overline{\Delta \omega_k^2} = \sum_{\xi} (U_{\xi}^{(k)})^2 (-\epsilon_\xi \omega^2 \gamma_\xi). \quad (21)$$

Calculating, as before, the erfc concentration profile and replacing the sum in (21) by an integral we obtain

$$\overline{\Delta \omega_k^2} = \frac{\alpha_s^2}{1 + \alpha_s^2} \epsilon_s \tilde{\omega}_k^2 L \frac{1}{\sqrt{\pi}} \left\{ 1 - [e^{-(k,L)^2}/k_s L] \int_0^{k,L} e^{z^2} dz \right\}. \quad (22)$$

If $k_s L \rightarrow 0$ (small mode indices), the term in brackets in (22) tends to $\frac{2}{3}(k_s L)^2$. So far, the modes of the different subbands move in opposite directions, and the shift increases parabolically with the mode number increase.

A similar result was obtained by Kechrakos and Inkson [5], who used the VCA. They applied their approach to GaAs/AlAs SL, which is not justified, as we saw above, and as was noticed in [8].

Fluctuations of the composition, with respect to the virtual crystal, lead to broadening of δ -like peaks of the phonon density of states. If the fluctuations are small enough to be approximated by a Gaussian distribution and to allow the locator fluctuations $\delta g_{kk'}$ to remain in the form of (16) in the representation (9) of the ideal SL, we can write for the confined optical phonons:

$$\langle G_{kk} \rangle = \frac{1}{\sqrt{\pi D_k}} \int \frac{g_{kk}}{1 + g_{kk} W_{kk}} e^{-\delta g_{kk}/2D_k} d(\delta g_{kk}) \tag{23}$$

where $g_{kk} = \bar{g}_{kk} + \delta g_{kk}$, \bar{g}_{kk} corresponds to the VCA, and $D_k = \langle \delta g_{kk}^2 \rangle$. Since it can be shown that

$$\begin{aligned} \langle (g_\xi - \bar{g}_\xi)^2 \rangle &= \epsilon_\xi \omega^4 \bar{g}_\xi^4 \langle \delta C_\xi^2 \rangle [1 + 2\epsilon_\xi \gamma_\xi \omega^2 \bar{g}_\xi + 3(\epsilon_\xi \gamma_\xi \omega^2 \bar{g}_\xi)^2 + \dots] \\ &= \left[\epsilon_\xi^2 \omega^4 \langle \delta C_\xi^2 \rangle / (\bar{g}_\xi^{-1} - \epsilon_\xi \gamma_\xi \omega^2)^2 \right] \bar{g}_\xi^2 \end{aligned} \tag{24}$$

we obtain, using (23) and (24):

$$\text{Im} \langle G_{kk} \rangle \sim \exp \left[-(\omega^2 - \bar{\omega}_k^2) / \epsilon^2 \omega_k^2 B_k \right] \tag{25}$$

where

$$B_k = \sum_\xi (U_\xi^{(k)})^4 \frac{\langle \delta C_\xi^2 \rangle}{(1 - \epsilon \gamma_\xi \omega_k^2 \bar{g}_{kk})^2} \tag{26}$$

In the case of non-correlated disorder, again replacing the sum in (26) by an integral, we find ($kL \rightarrow 0$):

$$B_k = (1/2\sqrt{2\pi}) [\alpha_s^2 / (1 + \alpha_s^2)]^2 (kL)^4 (L/N_p) \tag{27}$$

It follows from (25) and (27) that δ -like peaks at the squared frequencies of the confined phonon modes are broadening symmetrically into the Gaussian curve with a characteristic width proportional to the average shift:

$$\sqrt{\Delta E_k^2} \sim \Delta \omega_k^2 / LN_p$$

4. Conclusion

We can conclude that the character of the interfacial imperfection on the LO confined modes is rather different in the cases considered, with respect to both the mode shift and the 'shape of the line'. In the practically interesting case of AlAs/GaAs SL a simple formula (18) is obtained which allows one to estimate the shift easily.

We assumed that the fluctuations are coherent in different periods of the SL. In fact this is not so. The incoherence means: (i) fluctuations of the broadening length L ; (ii) an incoherence of the composition fluctuations with respect to periodical $\gamma(z)$.

The latter means that

$$\langle \delta C_{\xi}(Q - Q') \delta C_{\xi}(Q' - Q'') \rangle = \langle \delta C_{\xi}^2 \rangle \delta_{QQ''}$$

and does not lead to any change in the results above because the confined modes are independent of the SL wavenumber Q .

The fluctuations of L , which characterizes the average composition distribution in each period, may lead to an additional broadening of the modes. This depends on the particular technique of the SL fabrication. In fact, we did not consider any specific mechanism of the interfacial broadening, but if growth-process-dependent functions γ_{ξ} and $\langle \delta C_{\xi}^2 \rangle$ are known, it can be taken into account in an obvious way. On the other hand, spectroscopy of the confined LO modes can be an instrument for characterization of the correlation effects in the impurity distribution both in plane and between the planes.

Acknowledgments

The author is grateful to T Dumelow, B Samson and S R P Smith for helpful discussions. He would also like to acknowledge financial support from the British Council.

References

- [1] Levi D *et al* 1987 *Phys. Rev. B* **36** 8032
- [2] Fasol G *et al* 1988 *Phys. Rev. B* **38** 6056
- [3] Jusserand B *et al* 1990 *Appl. Phys. Lett.* **57** 560
- [4] Jusserand B 1990 *Phys. Rev. B* **42** 7256
- [5] Kechrakos D and Inkson J C 1990 *Proc. 20th Int. Conf. on Physics of Semiconductors (Thessalonika, 1990)* (Singapore: World Scientific) p 1449
- [6] Jusserand B and Mollot F 1990 *Proc. 20th Int. Conf. on Physics of Semiconductors (Thessalonika, 1990)* (Singapore: World Scientific) p 1985
- [7] Baroni S, Gianozzi P and Molinari E 1990 *Phys. Rev. B* **41** 3870
- [8] Samson B *et al* 1991 *Solid State Commun.* **78** 325
- [9] Ziman J M 1979 *Models of Disorder* (Cambridge: Cambridge University Press)
- [10] Albuquerque E L, Fulco P and Tilley D R 1988 *Phys. Status Solidi b* **146** 449
- [11] Lifshitz I M, Gredeskul S A and Pastur L A 1982 *Introduction to Theory of Disordered Systems* (Moscow: Nauka)
- [12] Taylor D W 1988 *Optical Properties of Mixed Crystals* ed R J Elliott (Amsterdam: North-Holland) pp 35-130
- [13] Strauch D and Dorner B 1990 *J. Phys.: Condens. Matter* **2** 1457
- [14] Baroni S, Gironcoli S and Gianozzi P 1990 *Phys. Rev. Lett.* **65** 84